Tree Physiology 38, 1180–1192
doi:10.1093/treephys/tpy049

Research paper

Variations in xylem embolism susceptibility under drought between intact saplings of three walnut species

Thorsten Knipfer[1], Felipe H. Barrios-Masias[1,4], Italo F. Cuneo[1,5], Martin Bouda[2], Caetano P. Albuquerque[1], Craig R. Brodersen[2], Daniel A. Kluepfel[3] and Andrew J. McElrone[1,3,6]

[1]Department of Viticulture & Enology, University of California, Davis, CA 95616, USA; [2]School of Forestry and Environmental Studies, Yale University, New Haven, CT 06511, USA; [3]USDA-ARS, Crops Pathology and Genetics Research Unit, Davis, CA 95616, USA; [4]Present address: Department of Agriculture, Nutrition and Veterinary Sciences, University of Nevada, Reno, NV 89557, USA; [5]Present address: School of Agronomy, Pontificia Universidad Católica de Valparaíso, Quillota 2260000, Chile; [6]Corresponding author (ajmcelrone@ucdavis.edu)

Received August 18, 2017; accepted May 16, 2018; published online May 30, 2018; handling Editor Jordi Martinez-Vilalta

A germplasm collection containing varied *Juglans* genotypes holds potential to improve drought resistance of plant materials for commercial production. We used X-ray computed microtomography to evaluate stem xylem embolism susceptibility/repair in relation to vessel anatomical features (size, arrangement, connectivity and pit characteristics) in 2-year-old saplings of three *Juglans* species. In vivo analysis revealed interspecific variations in embolism susceptibility among *Juglans microcarpa*, *J. hindsii* (both native to arid habitats) and *J. ailantifolia* (native to mesic habitats). Stem xylem of *J. microcarpa* was more resistant to drought-induced embolism as compared with *J. hindsii* and *J. ailantifolia* (differences in embolism susceptibility among older and current year xylem were not detected in any species). Variations in most vessel anatomical traits were negligible among the three species; however, we detected substantial interspecific differences in intervessel pit characteristics. As compared with *J. hindsii* and *J. ailantifolia*, low embolism susceptibility in *J. microcarpa* was associated with smaller pit size in larger diameter vessels, a smaller area of the shared vessel wall occupied by pits, lower pit frequency and no changes in pit characteristics as vessel diameters increased. Changes in amount of embolized vessels following 40 days of re-watering were minor in intact saplings of all three species highlighting that an embolism repair mechanism did not contribute to drought recovery. In conclusion, our data indicate that interspecific variations in drought-induced embolism susceptibility are associated with species-specific pit characteristics, and these traits may provide a future target for breeding efforts aimed at selecting walnut germplasm with improved drought resistance.

Keywords: microCT, saplings, water relations, water stress, X-ray, xylem.

Introduction

Walnuts are an economically important crop worldwide, but production is often limited due to water scarcity. Farmers encounter increased pressure to optimize water-use efficiency, and in turn require plant genotypes that are able to better tolerate and maintain productivity under water deficit. Tree crops are commonly grafted onto rootstocks to confer resistance to a variety of abiotic and biotic stressors (Christensen 2003, DeJong et al. 2004). For example, wild *Juglans* species have been shown to possess potential to improve disease resistance via their use as rootstocks (Kluepfel et al. 2012), and may help to improve frost resistance in cold conditions (Charrier et al. 2011, 2017). However, work is still needed to evaluate the physiological responses of *Juglans* species to drought stress in relation to species-specific anatomical traits.

Water stress by drought induces air embolism in xylem conduits that block long-distance water transport and reduce water transport capacity from roots to a transpiring canopy (Tyree and Sperry 1989). Imaging techniques such as X-ray computed microtomography (microCT) enable direct observation of xylem embolism, and allow determination of embolism susceptibility/

repair in the intact plant (in vivo) (Brodersen et al. 2010, Knipfer et al. 2015*a*, 2015*b*, 2016, Charrier et al. 2016, Choat et al. 2016); thereby excluding artifacts related to organ excision as is necessary for hydraulic measurements of xylem vulnerability (Wheeler et al. 2013, Cochard et al. 2013, 2014, Torres-Ruiz et al. 2015). For *Juglans* species, observations of xylem embolism using microCT have been reported for *J. microcarpa* (drought stress, Knipfer et al. 2015*b*) and *J. regia* (freeze–thaw events, Charra-Vaskou et al. 2016). Using microCT on intact grapevines, we recently found that both drought-induced embolism susceptibility and repair following soil re-watering can differ among congeneric species (Knipfer et al. 2015*a*): *Vitis riparia* (mesic habitat) was more susceptible to embolism as compared with *Vitis champinii* (more arid habitat), and substantial embolism repair was only observed for *V. riparia*. Similarly, literature indicates that differences in embolism susceptibility under drought and repair exist among walnut species and suggests that (i) *Juglans microcarpa* is less vulnerable to embolism as compared with *J. regia* (Tyree et al. 1993, Knipfer et al. 2015*b*), (ii) *J. microcarpa* is unable to repair embolism following drought (Knipfer et al. 2015*b*) and (iii) winter embolism repair in *J. regia* is linked to cellular water transport facilitated by aquaporins (Sakr et al. 2003). However, current data do not provide direct evidence if that walnut species from varied habitats differ in embolism susceptibility under drought and embolism repair following soil re-watering under in vivo conditions.

Wood anatomy can differ among plant species (Carlquist 2001), and susceptibility to drought-induced embolism has been associated with anatomical features such as vessel size (Hargrave et al. 1994, McCulloh et al. 2012), intervessel connectivity (Brodersen et al. 2013, Knipfer et al. 2015*b*) and intervessel pit characteristics (Choat et al. 2003). Xylem resistance to drought-induced embolism in *J. microcarpa* appears to be related to high frequencies of smaller diameter vessels and low intervessel connectivity that restricts embolism spread to short files of multiple vessels and limits an extensive spread of air through the xylem network initiated from a single embolized vessel (Knipfer et al. 2015*b*). Whether vessel anatomical traits vary across *Juglans* species and to what extent these traits determine drought-induced embolism susceptibility remains to be investigated.

In this study, we used microCT imaging to investigate in vivo embolism susceptibility under drought and embolism repair following soil re-watering in 2-year-old saplings of three *Juglans* species (*J. microcarpa*, *J. hindsii*, *J. ailantifolia*). Our general hypotheses were that (i) *Juglans* species native to drier habitats have xylem vessels that are less susceptible to drought-induced embolism, (ii) differences in embolism susceptibility among *Juglans* species are linked to vessel anatomical traits and (iii) effective embolism repair following re-watering is species dependent (similar to results reported for grapevine species in Knipfer et al. 2015*a*). Saplings were obtained from the USDA-ARS Germplasm collection in Davis, CA, USA. In vivo investigations were complimented with microCT-based anatomical analyses of vessel size, intervessel connectivity and pit characteristics, as well as measurements of leaf stomatal conductance and root pressure.

Materials and methods

Plant material

Investigations were performed on three walnut species (*J. microcarpa*, *J. hindsii*, *J. ailantifolia*) that occur over a broad range of habitats in North America (see Figure S1 available as Supplementary Data at *Tree Physiology* Online; Aradhya et al. 2007). Of the three species, *J. hindsii* is already used as a commercial rootstock that provides resistance to 'crown gall disease'. Walnut saplings of *J. microcarpa*, *J. hindsii* and *J. ailantifolia* were grown from seed in 0.5-l pots filled with a soil mixture (40% washed sand, 20% sphagnum peat moss, 20% redwood compost, 20% pumice rock) at the USDA-ARS Germplasm Repository in Davis, CA, USA. Growth of saplings was maintained under ambient atmospheric conditions [average monthly low/high temperature of ~7/34 °C (March to September) and ~3/26 °C (October to February)] at the Germplasm Repository for ~2 years, and saplings were watered regularly. Two months prior to analyses, saplings were moved to an environmentally controlled greenhouse at UC Davis, CA, USA (day/night temperature of ~25/8 °C, photoperiod of ~15 h, relative humidity of ~35%) and watered twice daily to keep the soil fully hydrated with water supplemented with macro- and micro-nutrients (Knipfer et al. 2015*a*). To study the impact of water stress by drought and re-watering on sapling hydraulics, saplings of each species were analyzed after they were subjected to four irrigation treatments in the greenhouse: (i) well-watered (stem water potential, Ψ_{stem}, >−1 MPa), (ii) moderately water stressed under drought (Ψ_{stem} at −1 to −3 MPa), (iii) severely water stressed under drought (Ψ_{stem} at −3 to −4 MPa) and (iv) re-watered following moderate stress. Saplings were subjected to drought stress by eliminating watering for several days (2–7 days) prior to analysis with the duration of drought stress depending on the targeted Ψ_{stem}. Re-watered saplings were maintained at full soil moisture under greenhouse conditions. At the time of the experiments, saplings had an average height of 0.74 m (*J. microcarpa*, range 0.56–1.05 m), 0.83 (*J. hindsii*, 0.48–1.0 m) and 0.64 m (*J. ailantifolia*, 0.37–0.90 m), and had an average leaf surface area of 718 cm^2 (*J. microcarpa*, range 451–940 cm^2), 573 cm^2 (*J. hindsii*, 381–866 cm^2) and 1521 cm^2 (*J. ailantifolia*, 1241–2235 cm^2) (see examples in Figure S1B available as Supplementary Data at *Tree Physiology* Online). Experiments on intact saplings were performed in the year 2015 between the calendar month April and May.

Stem water potential (Ψ_{stem})

Plant water status was determined by measuring Ψ_{stem} with a Scholander pressure chamber (Soil Moisture Equipment Corp 3005, Goleta, CA, USA). Leaves were covered and sealed with a foiled plastic bag for 20–30 min prior to measurement. Leaflets were then excised at the base of the petiolule with a sharp razor blade and placed into the chamber with the petiolule end protruding out of the sealed chamber. The chamber was slowly pressurized, and the pressure (balancing pressure) at which water started to emerge from the transverse surface of the cut end was recorded (i.e., Ψ_{stem}). For measurement of Ψ_{stem}, it was assumed that a hydraulic continuum between bagged leaflet and stem xylem existed at time of analysis for saplings of all species, despite the distance between the two organs and potential segmentation of xylem; in theory, the symplast of a bagged leaf will eventually equilibrate with stem xylem pressure even if only a few functional vessels are present in the leaf (i.e., not hydraulically isolated from stem) at time of measurement (balancing pressure = $\Psi_{symplast} = \Psi_{stem}$ = stem xylem pressure).

X-ray computed microtomography (microCT)

Intact walnut saplings were imaged at the microCT facility (beamline 8.3.2) at the Lawrence Berkley National Laboratory Advanced Light Source (ALS) (see details in Brodersen et al. 2010, McElrone et al. 2013, Knipfer et al. 2015*a*, 2015*b*). Groups of replicate saplings (n = 3–5 of each species) subjected to well-watered, moderately watered stressed and severely water stressed conditions (as described above) were transported from the greenhouse to ALS within 1.5 h by car, stored at beamline 8.3.2 under low light laboratory conditions and imaged randomly within experimental blocks within 24 h of arrival. Sapling Ψ_{stem} (as measured on a bagged leaflet at canopy level) was determined <15 min prior to imaging and subsequently the pot of the sapling was fixed in a custom-made aluminum cage that was placed on a rotating stage. A 1- to 5-mm section of the stem just above the soil was imaged in the 23 keV synchrotron X-ray beam as the sapling rotated continuously. The time period of imaging was ~10 min and yielded 1025 longitudinal 2-D images with a 3.2 μm pixel resolution captured on a CMOS camera (PCO.edge; PCO, Kehlheim, Germany). Several saplings subjected to water stress by drought were re-watered, transported back to the greenhouse, and imaged again after 40 days (n = 2–4 of each species); two additional saplings were only scanned after 40 days of re-watering to check if embolism repair was compromised by X-ray exposure. Following imaging and detection of embolized vessels in vivo, the stem portion including the scanned location was excised (~4 cm in length), dehydrated for 5 days at 30 °C, and imaged again at 3.2 μm pixel resolution for analysis of total population of vessels, vessel dimensions and intervessel connectivity, and at 0.65 μm pixel resolution for analysis of pit characteristics (see below). 2-D longitudinal raw images were reconstructed into a stack of transverse images using a custom software plug-in for Fiji imaging software (www.fiji.sc, ImageJ) that used Octopus 8.3 Software (Institute for Nuclear Sciences, Ghent University, Ghent, Belgium) in the background. Vessel number and diameter were measured using a semi-automated routine in Fiji imaging software (www.fiji.sc, ImageJ): First, the cross-sectional area of each vessel was labeled manually using the 'Brush' tool, then vessel number was calculated automatically using the 'Analyze Particle' tool, and corresponding vessel diameter was calculated by $d = \sqrt{(A/\pi)} \times 2$. The percentage of embolized vessels was determined by (number of embolized vessels/total number of vessels) × 100%. In addition, diameter distribution profiles for either the total populations of vessels (as obtained from dehydrated stem segments) or exclusively embolized vessels (as obtained in vivo) were generated for diameter size classes of 0–5, 5–10, …, 80–85 μm, and vessel frequency for each size class was determined by (number of vessels per size class/total number of vessels) × 100% (for details see Knipfer et al. 2015*b*).

Vessel connectivity and arrangement

Intervessel connectivity and vessel arrangement was analyzed from dehydrated stem segments imaged at 3.2 μm pixel resolution. For a representative section of the xylem, binary image labels for vessel lumina were subjected to image analysis in MATLAB (MATLAB version 8.5, 2015, The MathWorks Inc., Natick, MA). Lumina of individual vessels were separated out by an 8-neighborhood contiguity algorithm, and spots in binary images comprising fewer than 10 contiguous pixels were eliminated to minimize image artifacts during image processing. The minimum intervessel distance for all vessel pairs in which the centers were separated by <150 μm (plus the two vessels' diameters) was detected by checking the pairwise distances between all the respective vessels' edge pixels (i.e., an edge pixel is any vessel lumen pixel adjacent to a non-lumen pixel). 'Interconnected' vessels were separated by a distance that was less than the measured average thickness of the shared double-wall containing intervessel pits (<12 μm in all three species as determined from microCT images); in turn, a 'solitary' vessel was isolated from all neighboring vessels by ≥12 μm. In addition, a 'vessel grouping' was defined as a set of vessels that was interconnected. Based on these parameters, we determined the intervessel connectivity index (IVC = N connections/N vessels) and vessel grouping indices (F_{VM} = N groupings/N vessels; V_G = N vessels/(N groupings + N solitary vessels)) (for review see Scholz et al. 2013).

Pit characteristics

Dehydrated stem segments were imaged at higher spatial resolution of 0.65 μm per pixel (resolution limit of 0.42 μm^2) in order to more closely investigate intervessel pit characteristics. Following reconstruction of 2-D projections into a stack of transverse images, images were loaded into the software AVIZO 8.0

(VSG, FEI Company, Hillboro, OR, USA) and vessel lumina were reconstructed in 3-D using the 'edit label field' module, and 3-D volume renderings were generated using the 'volume rendering' module (Knipfer et al. 2016). Using the 'slice' tool in AVIZO, the lumen of a vessel that shared a double-wall with a neighboring vessel was sliced open in tangential direction. This revealed the anatomical structure of the shared vessel wall ($A_{shared\text{-}wall}$). Subsequently, an image of the 3-D volume rendering was acquired and uploaded into Fiji imaging software (see Figure S2A available as Supplementary Data at *Tree Physiology* Online). Using Fiji software, $A_{shared\text{-}wall}$ of each vessel element was determined using the 'polygon' tool, diameters were determined using the 'line' tool and averaged, and the 'brush' tool was used to label manually the area of intervessel pits (see Figure S2B available as Supplementary Data at *Tree Physiology* Online); a binary image of exclusively the intervessel pit area was generated using the 'image adjust – window/level' and 'process binary – make binary' tool (see Figure S2C available as Supplementary Data at *Tree Physiology* Online). The size of each intervessel pit opening (A_{pit}), the vessel wall area covered by pit openings ($A_{intervessel\ pits}$) and the number ($N_{intervessel\ pits}$) of intervessel pits was determined using the 'Analysis particle' tool. The percentage of $A_{shared\text{-}wall}$ covered by vessel-to-vessel pits was determined by ($A_{intervessel\ pits}/A_{shared\text{-}wall}$) × 100%, the average intervessel pits size of each vessel element was determined from ($\sum A_{pit}/N_{intervessel\ pits}$), and an estimate of the frequency of how many intervessel pits are present on a given area of the shared vessel wall was obtained by ($N_{intervessel\ pits}/A_{shared\text{-}wall}$).

Leaf gas exchange

Leaf stomatal conductance was measured midday between 11:00 and 13:00 h using a portable gas exchange system (Li-1600, Li-Cor, Inc., Lincoln, NE, USA). Measurements were performed in the greenhouse on the same day on replicate plants (n = 4–6 of each species) that had been subjected to well-watered, moderately stressed by drought and re-watered (for 5 days) conditions (as described above). For each sapling, non-shaded and mature leaves from the top of the canopy were measured and Ψ_{stem} was determined within 30 min of measurement of stomatal conductance.

Root pressure

Root pressure was measured under laboratory conditions (at around 24 °C) on re-watered saplings that were maintained in the greenhouse for 40 days following microCT analysis. The stem of the sapling was excised under water with pruning scissors about 3 cm above the soil, and the remaining stem portion of the root-system was attached to a 2 cm piece of semi-rigid tubing connected to a pressure transducer (for details see Knipfer et al. 2015*a*). During sample preparation, root-systems remained in the pot filled with soil. Subsequently, the soil was saturated and maintained at maximum water holding capacity during the time of root pressure recordings. The generation of root pressure in this 'closed-system' is directly linked to the ability of the root system to produce xylem exudate (Knipfer and Fricke 2010, Wegner 2013).

Data analysis

Quantitative analysis of data was performed using SAS (version 9.2, SAS Institute, Cary, NC, USA), and graphs were generated using SigmaPlot (version 8.0, Systat Software Inc., San Jose, CA, USA). Mean values and standard errors were determined using the 'PROC MEANS' procedure in SAS. Statistical differences were determined by analysis of variance (ANOVA) or covariance (ANCOVA) using the 'PROC GLM' procedure in SAS. For Table 1 and Figure 8, data were analyzed using a two-way ANOVA in a completely randomized design with species and water treatment as factors; Shapiro–Wilk test was used to evaluate data for normal distribution, Levene test was used to evaluate homogeneity of variance and Tukey–Kramer HSD test was used to determine significant differences at $P < 0.05$ (for P-values corresponding

Table 1. Summary of stem water potential (Ψ_{stem}) and corresponding percentages of embolized vessels of total vessels (%-embolism) in intact walnut saplings subjected to different watering treatments (watered daily, moderate stress by drought at Ψ_{stem} >−3 MPa following no irrigation, severe stress by drought at Ψ_{stem} <−3 MPa following no irrigation). Data are given as mean ± SE of n = 3–5 (range from minimum to maximum) saplings. Different letters indicate significant differences at $P < 0.05$ among means of Ψ_{stem} (letters 'A' to 'D') or %-embolism (letters 'X' to 'Z') (post hoc Tukey–Kramer test) for combination of all levels across variables. Total vessel number was 676 ± 36 (mean ± SE) in *J. microcarpa*, 792 ± 54 in *J. hindsii* and 1164 ± 82 in *J. ailantifolia*.

	J. microcarpa		*J. hindsii*		*J. ailantifolia*	
Treatment	Ψ_{stem} (MPa)	Embolism (%)	Ψ_{stem} (MPa)	Embolism (%)	Ψ_{stem} (MPa)	Embolism (%)
Watered	-0.4 ± 0.2^{A}	9 ± 9^{Z}	-0.3 ± 0.1^{A}	7 ± 4^{Z}	-0.4 ± 0.1^{A}	30 ± 9^{YZ}
	(−0.2 to −0.8)	(0 to 28)	(−0.2 to −0.5)	(1 to 16)	(−0.2 to −0.7)	(3 to 44)
Moderately stressed	-2.5 ± 0.1^{BC}	17 ± 5^{Z}	-2.4 ± 0.1^{BC}	23 ± 8^{Z}	-2.0 ± 0.3^{B}	59 ± 8^{XY}
	(−2.3 to −2.7)	(8 to 25)	(−2.1 to −2.6)	(2 to 38)	(−1.5 to −2.8)	(37 to 73)
Severely stressed	-3.7 ± 0.2^{D}	28 ± 5^{YZ}	-3.2 ± 0.2^{CD}	40 ± 10^{XYZ}	-3.7 ± 0.3^{D}	70 ± 5^{X}
	(−3.1 to −4.0)	(19 to 39)	(−3.0 to −3.5)	(20 to 57)	(−3.0 to −4.0)	(64 to 81)

to Table 1, see Table S1 available as Supplementary Data at *Tree Physiology* Online).

Results

In vivo microCT analysis demonstrated that 2-year-old saplings of *J. microcarpa*, *J. hindsii* and *J. ailantifolia* differ in drought-induced embolism susceptibility, and re-watered saplings of all three species exhibited negligible embolism repair (Table 1, Figures 1 and 2; see Figure S3 unlabeled images, Table S1 available as Supplementary Data at *Tree Physiology* Online for *P*-values). Following maintenance of saplings under well-watered conditions, representative transverse microCT images of the stem show that embolized vessels were largely absent in *J. microcarpa* and *J. hindsii*, whereas many embolized vessels were present in both older and current-year xylem in *J. ailantifolia* (Figure 1 top row). Corresponding enlarged microCT images showed that the majority of both embolized and remaining water-filled vessels were embedded in a matrix composed of largely water-depleted xylem tissue (dark gray color) in all three species (Figure 2 top row). MicroCT data collected on replicate saplings indicated that percentages of embolized vessels (%-embolism) under well-watered conditions were on average 9% for *J. microcarpa*, 7% for *J. hindsii* and 30% for *J. ailantifolia* at comparable Ψ_{stem} (Table 1); these average were not significantly different across species ($P > 0.05$).

Under drought stress, representative microCT images show that many more embolized vessels formed in both older and current-year xylem of all three species (Figure 1 middle row, Figure 2 bottom row). For all three species, there was no significant intraspecific difference in embolism susceptibility between older and current year xylem under increasing drought stress ($P > 0.05$, Figure 3A–C). Given the growing conditions of plants subjected to moderate (Ψ_{stem} of >-3 MPa) stress by drought,

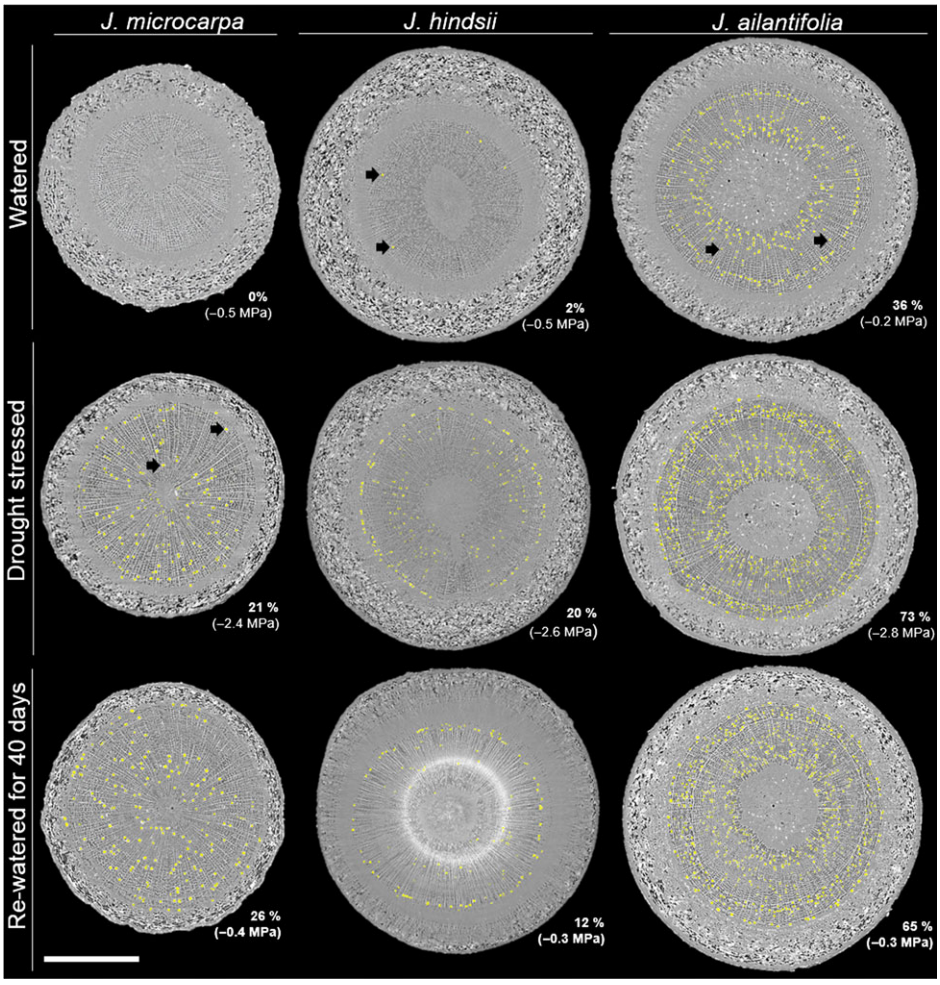

Figure 1. Representative transverse microCT images through the stem of intact saplings of three walnut species (*J. microcarpa*, *J. hindsii*, *J. ailantifolia*) subjected to different watering treatments. Air- and water-filled tissue appears in light and dark gray, respectively. The lumen of embolized vessels is labeled in yellow color for better visibility (see Figure S2 available as Supplementary Data at *Tree Physiology* Online for corresponding unlabeled images). Black arrows indicate examples of embolized vessels that occurred at great distance from other embolized vessels. Embolized vessels were detected in older xylem and current-year xylem close to cambium; this was most pronounced in *J. ailantifolia*. Images in middle and bottom row were acquired from the same sapling of each species. Values are percentage of embolized vessels (of total vessels) and Ψ_{stem}. Scale bar = 2 mm.

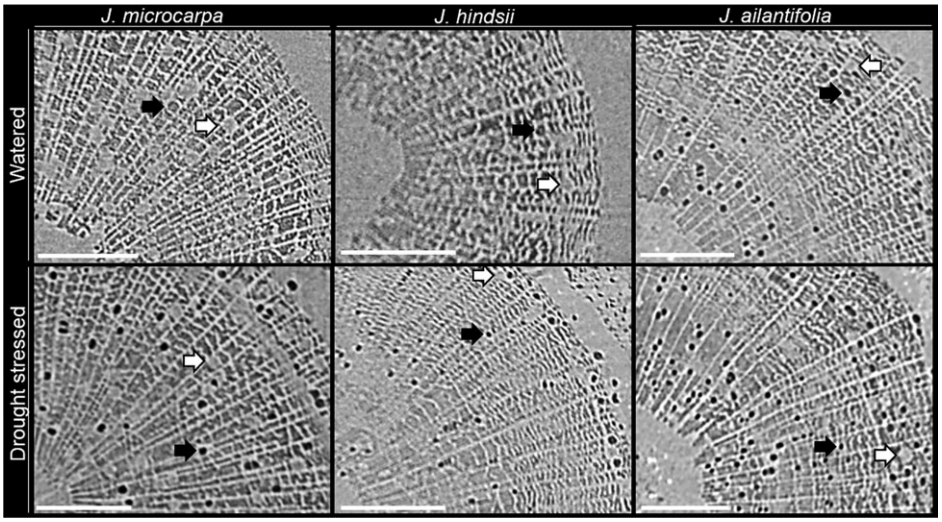

Figure 2. Enlarged transverse microCT images corresponding to Figure 1. Images provide a magnified view of stem xylem tissue under in vivo conditions. Air- and water-filled tissue appears in dark and light gray, respectively. White and black arrows indicate examples of water- and air-filled vessels, respectively, surrounded by largely air-filled (dark gray) xylem tissue. Scale bar = 500 μm.

average %-embolism was significantly higher for *J. ailantifolia* (59%) as compared with *J. microcarpa* (17%, $P = 0.02$) and *J. hindsii* (23%, $P = 0.04$) (Table 1). Under severe (Ψ_{stem} of < -3 MPa) stress, average %-embolism was 70% for *J. ailantifolia* and only 28% for *J. microcarpa* ($P = 0.02$) (Table 1). Following adjustment for initial %-embolism under non-stress conditions, the Ψ_{stem} threshold for 50% embolism was ~−4 MPa for *J. ailantifolia* and *J. hindsii* and −8 MPa for *J. microcarpa* (Figure 3D)

After maintenance of drought-stressed saplings under re-watered conditions for 40 days, microCT images showed that embolized vessels were still present at similar levels even after the extended re-watering period (Figure 1 bottom row). In saplings of all three species, a recovery in Ψ_{stem} was observed, but reductions in %-embolism were minimal or non-existent (by <10% in eight out of nine saplings). For saplings of *J. microcarpa*, %-embolism was reduced slightly in two saplings (by ~5% on average) while other saplings of this species exhibited a slight increase in %-embolism (by ~7% on average). Similar data were obtained for saplings of *J. hindsii* and *J. ailantifolia*. For *J. hindsii*, %-embolism was reduced by 2% on average across the saplings, while %-embolism was reduced by <1% in *J. ailantifolia* saplings. In saplings that were subjected to drought, but only scanned once following the re-watering period, similarly high values of embolized vessels were still present (*J. microcarpa*, 34%; *J. ailantifolia*, 47%) suggesting that embolism repair was not compromised by X-ray exposure in the plants scanned multiple times. Moreover, in all three species, root systems of re-watered saplings failed to produce xylem exudate following de-topping and in turn did not generate root pressure.

Vessel size distribution profiles for stem xylem differed slightly among saplings of the three species (Figure 4). For the entire population of vessels, saplings of *J. ailantifolia* and *J. microcarpa* had a greater frequency of vessels in larger diameter classes (30–35 μm), while *J. hindsii* had a greater frequency of vessels in smaller diameter classes (20–25 μm, >20% of vessels) (Figure 4). For *J. hindsii* and *J. microcarpa*, larger diameter vessels embolized more frequently under moderate stress (Ψ_{stem} >−3 MPa) and smaller diameter vessels embolized mainly under severe (Ψ_{stem} <−3 MPa) stress conditions (Figure 4); this shift in vessel profiles was most pronounced for *J. microcarpa* and absent for *J. ailantifolia*.

Analysis of transverse microCT image slices indicated that most vessels in stem xylem were solitary for all three species (on average 87% of solitary vessels in *J. microcarpa*, 87% in *J. hindsii* and 86% in *J. ailantifolia*; Table 2); the intervessel connectivity index (IVC) was on average ~0.07 and comparable between species ($P > 0.05$). Similarly, average values of vessel grouping indices (F_{VM} and V_G) were comparable between species ($P > 0.05$) indicating that differences in vessel arrangement among species were negligible (Table 2); average vessel density tended to be highest for *J. ailantifolia* (74 vessels mm^{-2}), intermediate for *J. hindsii* (66 vessels mm^{-2}) and lowest for *J. microcarpa* (56 vessels mm^{-2}); however, these values were not significantly different between species. The corresponding spatial arrangement of solitary and interconnected/grouped vessels is illustrated in 3-D for representative vessels of all three species (Figure 5, distance of around 600 μm between top and bottom transverse slice). 3-D data show that vessels identified as solitary or interconnected in a single transverse slice typically remained in this position along the axial distance of the microCT scan in all three species; some vessels identified as solitary here may connect to other vessel at further distances along the stem.

Intervessel pit characteristics differed among the three species (Figures 6 and 7). Representative 3-D volume renderings of microCT images show that intervessel pits located in the wall

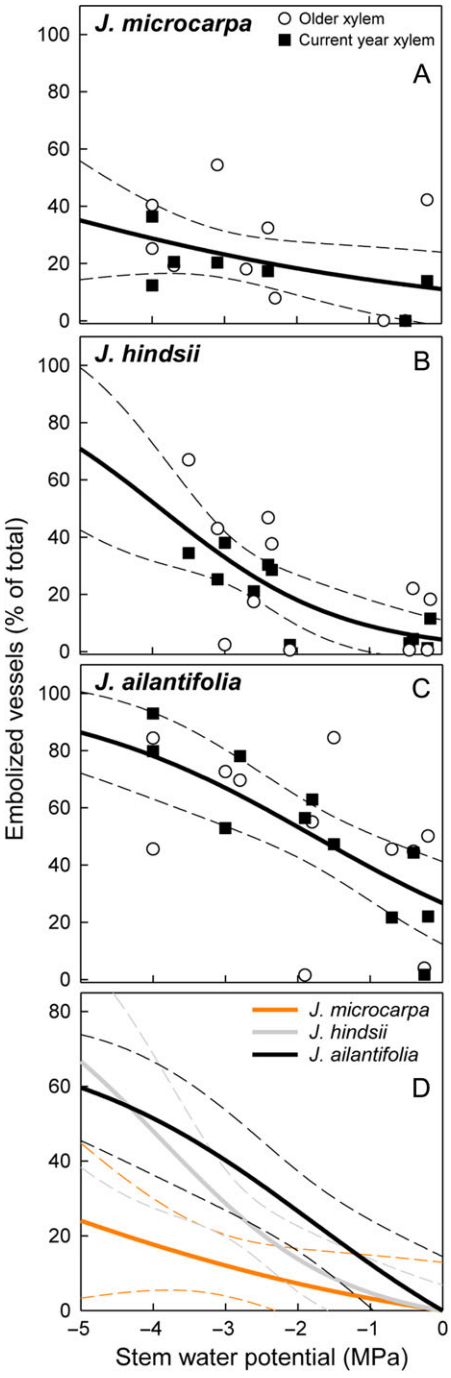

Figure 3. Relationship of Ψ_{stem} and %-embolism under increasing water stress by drought for stem xylem in intact saplings of (A) *J. microcarpa*, (B) *J. hindsii* and (C) *J. ailantifolia*. Within each species, ANOVA analyses predicted no significant difference among xylem regions for all three species (interaction of 'region*Ψ_{stem}' (independent variables) on '%-embolism' (dependent variable) at $P = 0.96$ for *J. microcarpa*, $P = 0.89$ for *J. hindsii*, and $P = 0.22$ for *J. ailantifolia*). (A–C) Solid lines are sigmoid nonlinear regressions fitted across data points of older and current year xylem (*J. microcarpa*, $b = -3.4$, $x_O = -7.1$, $R^2 = 0.42$, $P = 0.09$; *J. hindsii*, $b = -1.2$, $x_O = -3.9$, $R^2 = 0.67$, $P < 0.01$; *J. ailantifolia*, $b = -1.8$, $x_O = -1.8$, $R^2 = 0.67$, $P < 0.01$); dashed lines are corresponding 95% confidence intervals. (D) Adjusted nonlinear regressions (solid lines) of A–C for initial %-embolism at $\Psi_{stem} = 0$ MPa; dashed lines are estimated 95% confidence intervals.

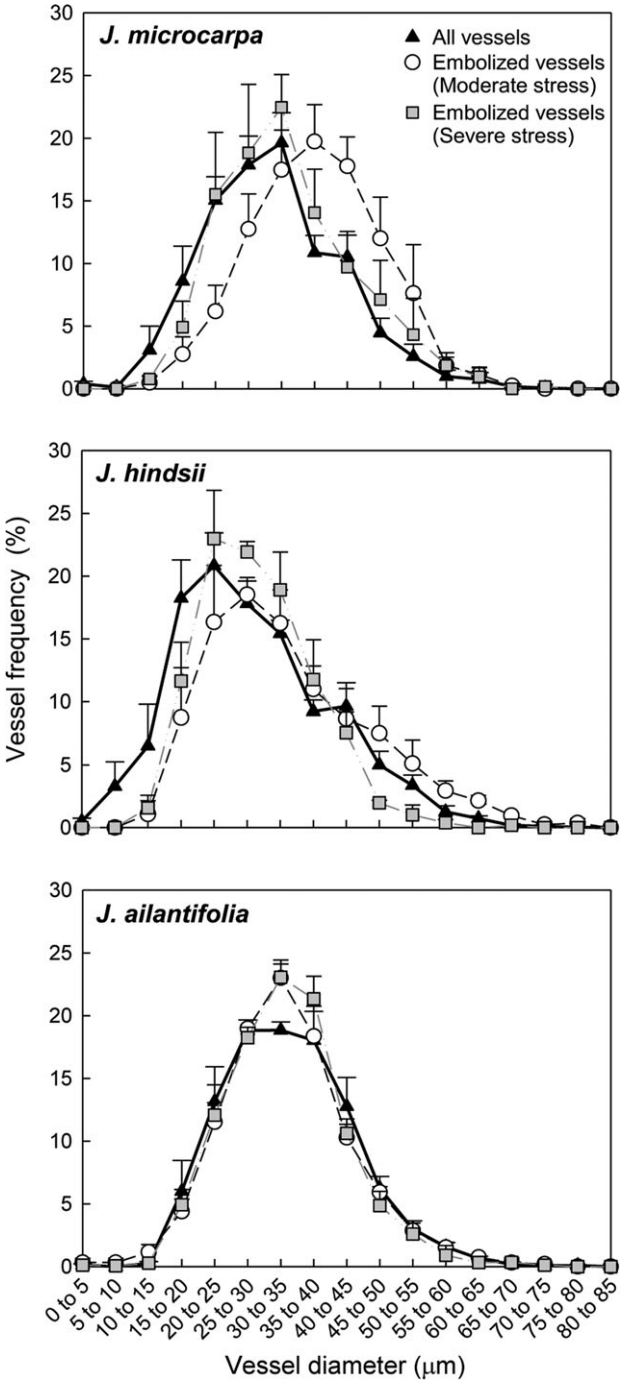

Figure 4. Vessel diameter distribution profiles in stem xylem of *J. microcarpa*, *J. hindsii* and *J. ailantifolia* saplings for the entire population of vessels ('all vessels') and exclusively for embolized vessels under moderate ($\Psi_{stem} > -3$ MPa) and severe (<−3 MPa) water stress by drought. Each data point is the mean ± SE ($n = 6$–8 saplings 'all vessels' and $n = 3$–4 'embolized vessels') in vessel frequency for a given diameter size class. Within one species, ANOVA analyses predicted an interaction of 'diameter*stress level' (independent variables) on 'frequency of embolized vessels' (dependent variable) at $P = 0.09$ for *J. microcarpa*, $P = 0.26$ for *J. hindsii* and $P = 0.97$ for *J. ailantifolia*.

between two neighboring vessels appeared to be smaller in size and occurred less frequently in *J. microcarpa* as compared with *J. ailantifolia* and *J. hindsii* (Figure 6). The estimated diameter of the pit ranged

Table 2. Vessel connectivity and arrangement in stem xylem of saplings from three walnut species as estimated from transverse microCT images. A xylem sector representing >30% of the xylem cross-sectional area (A_{xylem}) was evaluated; total A_{xylem} ranged from 7.9 to 19.9 mm^2 for *J. microcarpa*, 7.4 to 28.2 mm^2 for *J. hindsii* and 15.7 to 38.1 mm^2 for *J. ailantifolia*. Data are given as mean ± SE of $n = 6–9$ (range from minimum to maximum) saplings. ANOVA analysis indicated that none of the parameters were significantly different among species (P-values >0.05) (IVC = intervessel connectivity index, F_{VM} and V_G = vessel grouping indices).

Parameter	*J. microcarpa*	*J. hindsii*	*J. ailantifolia*
N vessels analyzed within xylem sector	183 ± 25 (63 to 224)	237 ± 23 (100 to 329)	357 ± 32 (259 to 484)
Solitary vessels (% of *N* vessels)	87 ± 3 (72 to 93)	87 ± 4 (65 to 98)	86 ± 4 (70 to 98)
IVC (*N* connections/*N* vessels)	0.070 ± 0.019 (0.036 to 0.156)	0.069 ± 0.022 (0.012 to 0.206)	0.076 ± 0.026 (0.01 to 0.168)
F_{VM} (*N* groupings/*N* vessels)	0.061 ± 0.014 (0.031 to 0.119)	0.058 ± 0.016 (0.012 to 0.150)	0.062 ± 0.019 (0.01 to 0.132)
V_G (*N* vessels/(*N* groupings + *N* solitary vessels))	1.077 ± 0.023 (1.037 to 1.185)	1.078 ± 0.027 (1.012 to 1.254)	1.087 ± 0.032 (1.011 to 1.202)
Vessel density (*N* vessels/A_{xylem} mm^2)	56 ± 11 (13 to 83)	66 ± 6 (40 to 93)	74 ± 9 (56 to 113)

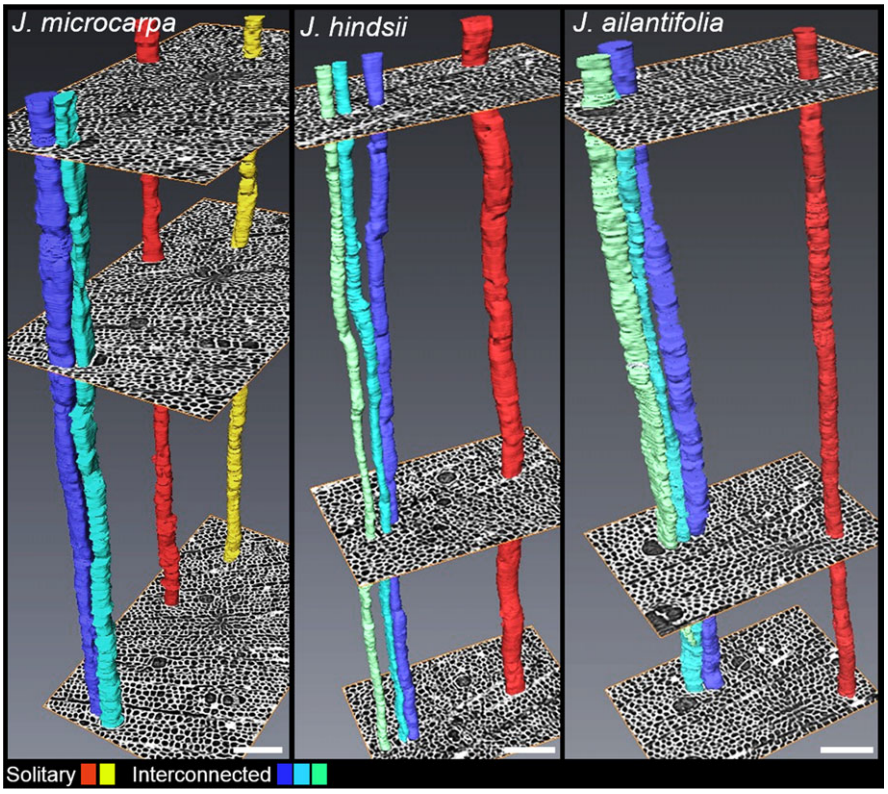

Figure 5. Representative 3-D reconstructions of vessels in stem xylem of saplings of three walnut species. Images were generated from microCT scans of dehydrated stems. Examples of vessels are shown that were either solitary (i.e., isolated from surrounding vessels) or interconnected (i.e., shared double wall with neighboring vessels) within the field of view. Scale ≈100 μm.

from 9 to 12 μm^2 for *J. microcarpa*, whereas pits of up to 25 μm^2 in size were detected in *J. hindsii* and *J. ailantifolia* (Figure 7A); pit size was significantly smaller in *J. microcarpa* as compared with *J. ailantifolia* ($P < 0.05$). Intervessel pits covered <16% of shared wall area ($A_{shared\text{-}wall}$) in *J. microcarpa*, which was substantially lower ($P < 0.05$) than in *J. hindsii* and *J. ailantifolia* (up to 35%, Figure 7B). Pit size and %-area covered by pits increased significantly with increasing diameter of vessel elements in *J. hindsii* and *J. ailantifolia*, but did not in *J. microcarpa* (Figure 7A and B). There was no relationship between ratio of ($N_{intervessel\ pits}$: $A_{shared\text{-}wall}$) and vessel diameter in all three species, but this ratio indicated that pit frequency (i.e., number of pits per $A_{shared\text{-}wall}$) was significantly ($P < 0.05$) lower in *J. microcarpa* as compared with *J. hindsii* and *J. ailantifolia* (Figure 7C).

Leaf gas exchange measurements indicated interspecific differences in stomatal conductance (Figure 8). Under well-watered conditions and comparable Ψ_{stem} (Figure 8A), stomatal conductance was around fourfold higher in *J. ailantifolia* as compared with *J. hindsii* ($P < 0.05$), while it was intermediate in *J. microcarpa*

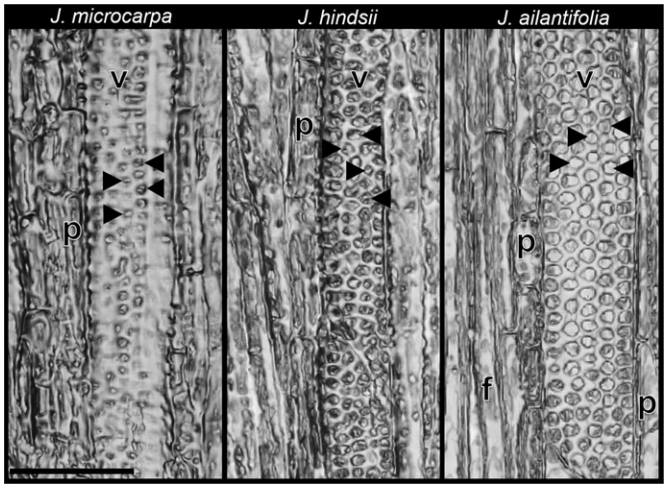

Figure 6. Representative 3-D renderings showing the anatomical structure of the shared vessel wall containing intervessel pits (examples indicated by arrows) for stem xylem of saplings of three walnut species. Images were generated from microCT images of dehydrated stem segments (v = vessel lumen, p = parenchyma cell, f = fiber). Scale bar = 50 μm.

(Figure 8B). Drought-induced reductions in stomatal conductance were substantial in saplings of *J. ailantifolia* ($P < 0.05$), and less severe in *J. microcarpa* and *J. hindsii* at comparable Ψ_{stem} (Figure 8B). In saplings following 5 days of re-watering, Ψ_{stem} values were comparable to well-watered conditions in all three species (Figure 8A). In re-watered saplings of *J. ailantifolia* stomatal conductance remained at a significantly lower level than in well-watered saplings (Figure 8B), whereas stomatal conductance in re-watered saplings of *J. microcarpa* reached a similar level than in well-watered saplings (Figure 8B); there was no indication for recovery in stomatal conductance in saplings of *J. hindsii*.

Discussion

This study provides novel insights into variations in xylem embolism susceptibility among walnut species (*J. microcarpa*, *J. hindsii*, *J. ailantifolia*) under in vivo conditions. When subjected to water stress, intact saplings of *J. micrcocarpa* (native to an arid habitat) were most resistant to drought-induced embolism and saplings of *J. ailantifolia* were least resistant (native to a mesic habitat). Our data suggest that the observed interspecific variation in embolism susceptibility was associated primarily with differences in intervessel pit characteristics between species, whereas interspecific differences in other vessel anatomical traits were less prominent (vessel size) or absent (vessel connectivity and arrangement). Following re-watering, effective embolism repair was not detected for any of the *Juglans* species, unlike for *Vitis* species where this process was most pronounced in *V. riparia* as native to mesic habitats (Knipfer et al. 2015*a*).

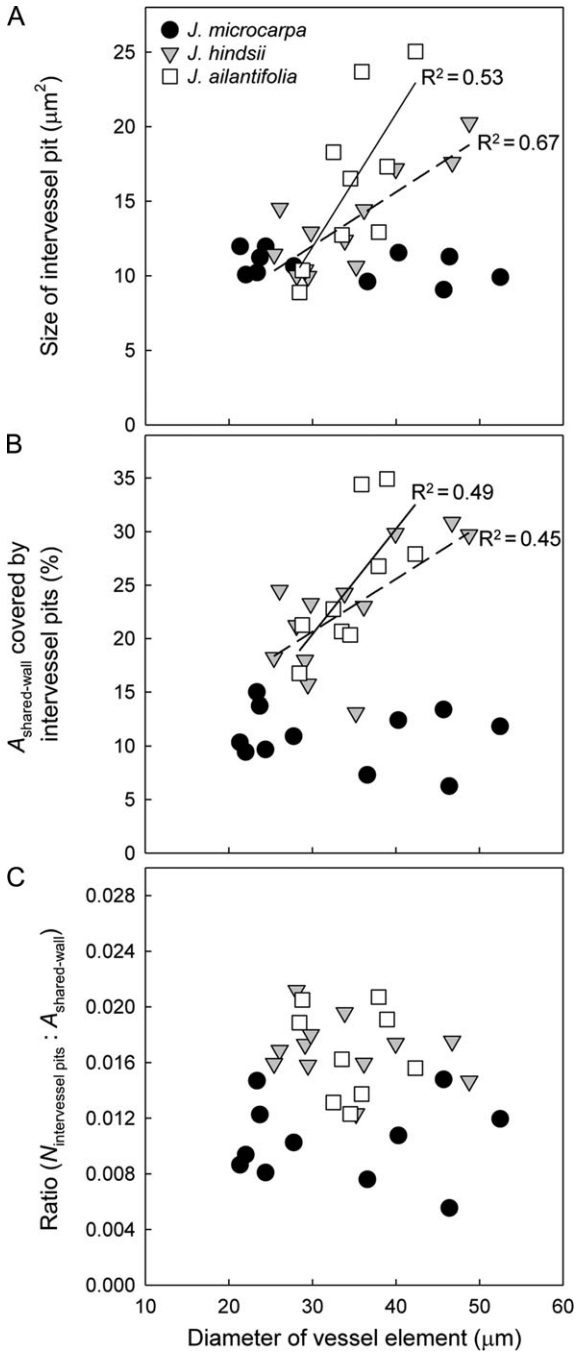

Figure 7. Intervessel pit characteristics in stem xylem of three walnut species as analyzed from microCT images (as shown in Figure 6). (A) intervessel pit size, (B) %-area of shared vessel wall ($A_{shared\text{-}wall}$) covered by intervessel pits and (C) ratio of number of intervessel pits per $A_{shared\text{-}wall}$. Data show that in *J. microcarpa* intervessel pits were generally of smaller size and less frequent for various vessel diameters, in contrast to *J. hindsii* and *J. ailantifolia*. Linear regression lines are shown for significant ($P < 0.05$) relationships (dashed, *J. hindsii*; solid, *J. ailantifolia*). ANCOVA analysis (covariate 'diameter of vessel element') predicted the following *P*-values for comparison of (A) *J. microcarpa* and *J. ailantifolia* ($P < 0.01$), *J. microcarpa* and *J. hindsii* ($P = 0.07$), *J. hindsii* and *J. ailantifolia* ($P = 0.09$); (B) *J. microcarpa* and *J. hindsii* or *J. ailantifolia* ($P < 0.001$), *J. hindsii* and *J. ailantifolia* ($P = 0.29$); (C) *J. microcarpa* and *J. hindsii* or *J. ailantifolia* ($P < 0.001$), *J. hindsii* and *J. ailantifolia* ($P = 0.89$).

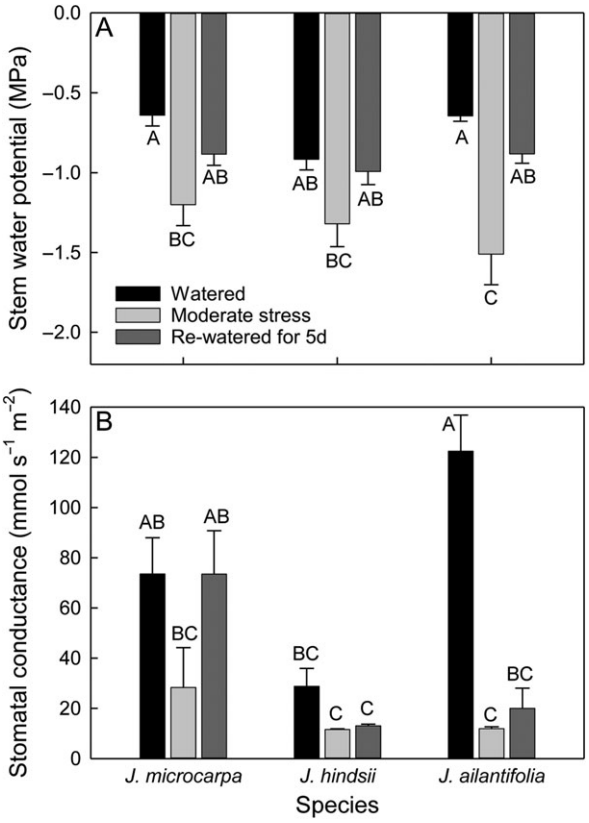

Figure 8. Midday (A) stem water potential and corresponding (B) stomatal conductance of saplings of three walnut species. Groups of replicate saplings were analyzed when subjected to different watering treatments (well-watered, moderately stressed under drought at Ψ_{stem} >−3 MPa, re-watered following moderate stress). Each bar is the mean ± SE of n = 4–6 saplings analyzed. Different letters 'A', 'B' and 'C' above the bars indicate significant differences between means ($P < 0.05$, post hoc Tukey–Kramer test).

Embolism formation under drought

Embolism susceptibility under drought has been found to be related to vessel size (Hargrave et al. 1994, McCulloh et al. 2012, Knipfer et al. 2015*b*) and intervessel pit characteristics (e.g. Choat et al. 2003, Jansen et al. 2009, Lens et al. 2011). Our current in vivo data indicate that slight differences in vessel size distributions exist among walnut species, but vessel size did not solely explain interspecific variations in embolism susceptibility. Intervessel pits facilitate the movement of water between vessels, and depending on their structural characteristics they can also allow for spread of air from an embolized to a functional vessel and in turn affect drought-induced embolism susceptibility (e.g. Tyree and Sperry 1989, Choat et al. 2003). Intervessel pit characteristics can vary among species, and pit membrane thickness was found to play a dominant role in drought-induced embolism susceptibility of woody plants (Jansen et al. 2009, Lens et al. 2011). Moreover, pit characteristics can also vary within a plant. The 'rare pit hypothesis' states that intervessel pits with membrane pores of air-seeding size are rare, but a higher pit number per vessel increases the likelihood of the presence of a 'leaky' pit to air that in turn increases a vessel's susceptibility to embolism (Choat et al. 2003, Wheeler et al. 2005, Christman et al. 2009). In this study we did not determine pit membrane thickness, but we evaluated pit size and frequency based on high-resolution microCT images. This 3-D spatial analysis had to be performed on dry stem material, since in vivo scans did not provide sufficient resolution of vessel wall structure (absolute pit dimension, as quantified here, may slightly vary between dry vs in vivo conditions). As compared with *J. hindsii* and *J. ailantifolia*, our data indicated that low embolism susceptibility in *J. microcarpa* was associated with smaller pit size in larger diameter vessels (Figure 7A), a smaller area of the shared vessel wall occupied by pits (Figure 7B), lower pit frequency (i.e., number of intervessel pits on shared vessel wall, Figure 7C) and no changes in pit characteristics as vessel diameters increased (Figure 7A–C). Pits may stretch during xylem development (Choat et al. 2003), and this could explain the observed relationship of increases in pit size with vessel diameter in *J. hindsii* and *J. ailantifolia*. The absence of this pattern in *J. microcarpa* may be explained by increased vessel wall strength in this species resisting internal tissue forces. In summary, a combination of vessel size and pit characteristics impacted drought-induced embolism susceptibility, and it can be speculated that two different strategies for xylem embolism avoidance in *Juglans* species exist: (i) maintenance of vessels that have pits of relatively small size/openings and frequency across all vessel sizes (*J. microcarpa*) or (ii) higher frequencies of those vessels in which pit size is minimized (*J. hindsii*).

Embolism repair and root pressure

In vivo observations indicate that an efficient embolism repair mechanism following drought is absent in trees (*Sequoia sempervirens*, Choat et al. 2015; *J. microcarpa*, Knipfer et al. 2015*a*; *Laurus nobilis*, Knipfer et al. 2017). For *L. nobilis*, successful vessel refilling appears to require that xylem pressures approach zero (Hacke and Sperry, 2003), and in vivo data indicate that this may only be possible when humid environmental conditions persist during the re-watering period providing for non-transpiring conditions (Knipfer et al. 2017). It is generally understood that generation of root pressure relaxes xylem pressure or even induces positive pressure in xylem sap (Charrier et al. 2016). For walnut, positive root/xylem pressure in the field follows a strong seasonality with peaks occurring early in the year (January) before budbreak (Ewers et al. 2001, Ameglio et al. 2002). Our data indicate that re-watered saplings of all three walnut species did not generate root pressure when measured in the month of May. In turn, root pressure in *Juglans* spp. appears to play a minor role in facilitating embolism repair following drought-watering cycles in the growing season. Stomatal conductance during the re-watering period (i.e., period for potential embolism recovery) was not zero, and we speculate that, together with the absent of root pressure, xylem pressures in all three walnut species tested were still too negative as needed for vessel refilling/embolism repair. Grapevines remain

the lone woody plant for which embolism repair has been conclusively documented using multiple in vivo imaging techniques (Holbrook et al. 2001, Brodersen et al. 2010, Knipfer et al. 2015*b*). It seems that woody species other than grapevine are limited in embolism repair during the growing season, which may be linked to their relatively low abundance of living xylem parenchyma driving this repair process (see Knipfer et al. 2016 for living xylem in grapevine). Recovery of *J. regia* from freeze-induced embolism formations during the winter was found to be related to new xylem growth, root pressure formation and activity of xylem parenchyma (Ameglio et al. 2002, Sakr et al. 2003). So, while walnut species may have the functional anatomy capable of embolism repair related to the presence of vessel-associated parenchyma (Secchi and Zwieniecki 2013, Salleo et al. 2008), this process appears to be ineffective for drought recovery during the growing season.

Stomatal control

Drought-induced stomata closure and reductions in plant water loss by transpiration can reduce the risk of excessive xylem tensions that would lead to embolism formation and systemic spread (e.g. Sparks and Black 1999, Brodribb et al. 2003, Martorell et al. 2013, Knipfer et al. 2015*a*). Stomata regulation and xylem function appear to be coordinated traits and this coordination is most likely crucial for an effective maintenance of plant water balance (Brodribb et al. 2017). Stomata control appears to aid the prevention of extensive xylem cavitation during water stress in walnut (*Juglans regia* × *nigra*; Cochard et al. 2002), with measured values of stomatal conductance ranging from 150 (control) to 20 (stress) mmol s^{-1} m^{-2}. Our present study provides some evidence that a coordination of stomata and xylem function most likely extends to several *Juglans* species. For example, high stomatal conductance in *J. ailantifolia* under well-watered conditions was linked to the presence of larger diameter and thus more-conductive vessels in this species, which provide for more efficient water supply to a generally larger canopy. However, stomatal conductance in *J. ailantifolia* was reduced significantly under drought, which was related to a substantial accumulation of embolized vessels. We speculate that the irreversible loss in stomatal conductance as observed for *J. ailantifolia* was somehow linked to extensive drought-induced embolism and a lack of short-term (days) embolism repair following re-watering. On the other hand, *J. hindsii* exhibited the lowest values of stomatal conductance under well-watered conditions, which was associated with smaller diameter and thus less-conductive vessels. In this species, reduction of stomatal conductance under drought and accumulation of embolized vessels was less severe than in *J. ailantifolia*; however, the amount of embolized vessels in *J. hindsii* potentially reached a threshold too that did not allow for recovery in stomatal conductance and embolism repair was lacking. Our data suggest that *J. microcarpa* achieves a good balance between effective long-distance water transport and canopy transpiration under both well-watered and drought conditions; the recovery of stomatal conductance in this species following soil re-watering was most likely related to relatively small amounts of embolized vessels that formed under drought that in turn allowed for maintenance of sufficient long-distance water transport capacity (since embolism repair was lacking, see also Knipfer et al. 2015*b*). Moreover, it should be noted that the leaf area of saplings differed substantially across species at time of analysis (on average 718 cm^2 for *J. microcarpa*, 573 cm^2 for *J. hindsii* and 1521 cm^2 for *J. ailantifolia*), but saplings were grown in pots of the same size, which commonly resulted in a faster drydown (1–2 days) of *J. ailantifolia* saplings to reach a similar Ψ_{stem} compared with *J. hindsii* and *J. microcarpa*. Differences in leaf area across species led to different rates of overall plant water loss, but since we expect embolism to respond directly to Ψ_{stem} rather than drydown rate, we do not consider pot size and leaf area to have affected the observed amounts of embolized vessels in stem xylem. The possible contribution of leaf xylem embolism on decline in stomata conductance and repair across walnut species remains to be elucidated in the future.

Conclusions

Walnuts are grown commercially worldwide, and *Juglans* species native to varied habitats hold the potential of providing new rootstock material with improved resistance to drought. Using X-ray microCT, we investigated in vivo the effect of drought-induced water stress on stem xylem embolism susceptibility (and repair following re-watering) in relation to vessel anatomical traits in *Juglans* species. Among the species tested, saplings of *J. microcarpa* (arid habitat) were most resistant to drought-induced embolism. In comparison, *J. ailantifolia* (mesic habitat) appeared to be the most vigorous species under well-watered conditions (largest canopy and highest stomatal conductance) but was relatively susceptible to drought-induced embolism linked to the presence of vessels with increased pit size and frequency. Embolism repair following re-watering for 40 days was negligible in intact saplings of all three *Juglans* species. For *Juglans*, our preliminary study indicates that pit characteristics (among various other vessel anatomical traits) are a promising target to more efficiently screen *Juglans* germplasm collections for drought resistance and embolism susceptibility.

Supplementary Data

Supplementary Data for this article are available at *Tree Physiology* Online.

Acknowledgments

The authors thank C. Reyes for valuable feedback on an earlier version of the manuscript. Also, we kindly thank D. Parkinson and A. MacDowell for their assistance at the Lawrence Berkeley

National Laboratory Advanced Light Source beamline 8.3.2 microtomography facility. The Advanced Light Source is supported by the Director, Office of Science, Office of Basic Energy Sciences, of the US Department of Energy under contract no. DE-AC02-05CH11231.

Conflict of interest

None declared.

Funding

A.J.M. is supported by the USDA-ARS Sustainable Viticulture Production Systems CRIS Project 2032-21220-006-00, NP305 Crop Production. C.P.A. received funding through CAPES/Brazil and I.F.C. through the Katherine Esau Graduate fellowship program.

References

Ameglio T, Bodet C, Lacointe A, Cochard H (2002) Winter embolism, mechanisms of xylem hydraulic conductivity recovery and springtime growth patterns in walnut and peach trees. Tree Physiol 2: 1211–1220.

Aradhya MK, Potter D, Gao F, Simon JC (2007) Molecular phylogeny of *Juglans* (Juglandaceae): a biographic perspective. Tree Genet Genom 3:363–378.

Brodersen CR, McElrone AJ, Choat B, Matthews MA, Shackel KA (2010) The dynamics of embolism repair in xylem: in vivo visualizations using high-resolution computed tomography. Plant Physiol 154: 1088–1095.

Brodersen CR, McElrone AJ, Choat B, Lee EF, Shackel KA, Matthews MA (2013) In vivo visualizations of drought-induced embolism spread in *Vitis vinifera*. Plant Physiol 162:1–10.

Brodribb TJ, Holbrook NM, Edwards EJ, Gutierrez MV (2003) Relations between stomatal closure, leaf turgor and xylem vulnerability in eight tropical dry forest trees. Plant Cell Environ 26:443–450.

Brodribb TJ, McAdam SA, Carins Murphy MR (2017) Xylem and stomata, coordinated through time and space. Plant Cell Environ 40:872–880.

Carlquist S (2001) Vessel grouping. In: Timell TE (ed) Comparative wood anatomy – systematic, ecological, and evolutionary aspects of dicotyledon wood, 2nd ed. Springer, Germany, pp 46–49.

Charra-Vaskou K, Badel E, Charrier G, Ponomarenko A, Bonhomme M, Foucat L, Mayr S, Ameglio T (2016) Cavitation and water fluxes driven by ice water potential in *Juglans regia* during freeze-thaw cycles. J Exp Bot 67:739–750.

Charrier G, Bonhomme M, Lacointe A, Ameglio T (2011) Are budburst dates, dormancy and cold acclimation in walnut trees (*Juglans regia* L.) under mainly genotypic or environmental control? Int J Biometeorol 55:763–774.

Charrier G, Torres-Ruiz JM, Badel E et al. (2016) Evidence for hydraulic vulnerability segmentation and lack of xylem refilling under tension. Plant Physiol 172:1657–1668.

Charrier G, Chuine I, Bonhomme M, Ameglio T (2017) Assessing frost damages using dynamics models in walnut trees: exposure rather than vulnerability controls frost risks. Plant Cell Environ 41:1008–1021.

Choat B, Ball M, Luly J, Holtum J (2003) Pit membrane porosity and water stress-induced cavitation in four co-exciting dry rainforest tree species. Plant Physiol 131:41–48.

Choat B, Brodersen CR, McElrone AJ (2015) Synchrotron microtomography of xylem embolism in *Sequoia sempervirens* seedlings during cycles of drought and recovery. New Phytol 205:1095–1105.

Choat B, Badel E, Burlett R, Delzon S, Cochard H, Jansen S (2016) Noninvasive measurement of vulnerability to drought-induced embolism by x-ray microtomography. Plant Physiol 170:273–282.

Christensen L (2003) Rootstock Selection. In: Christensen L, Dokoozlian NK, Walker MA, Wolpert JA (eds) Wine grape varieties in California. University of California Agricultural and Natural Resources Publication 3419, Oakland, CA, pp 12–15.

Christman MA, Sperry JS, Adler FR (2009) Testing the 'rare pit' hypothesis for xylem cavitation resistance in three species of *Acer*. New Phytol 182:664–674.

Cochard H, Coll L, Le Roux X, Ameglio T (2002) Unraveling the effects of plant hydraulics on stomatal closure during water stress in walnut. Plant Physiol 128:282–290.

Cochard H, Badel E, Herbette S, Delzon S, Choat B, Jansen S (2013) Methods for measuring plant vulnerability to cavitation: a critical review. J Exp Bot 64:4779–4791.

Cochard H, Delzon S, Badel E (2014) X-ray microtomography (micro-CT): a reference technology for high-resolution quantification of xylem embolism in trees. Plant Cell Environ 38:201–206.

DeJong TM, Johnson RS, Doyle TF, Basile B (2004) Growth, yield and physiological behavior of size-controlling peach rootstocks developed in California. Acta Hortic 658:449–455.

Ewers F, Ameglio T, Cochard H, Beaujard F, Martignac M, Vandame M, Bodet C, Cruiziat P (2001) Seasonal variation in xylem pressure of walnut trees: root and stem pressures. Tree Physiol 21:1123–1132.

Hargrave KR, Kolb KJ, Ewers FW, Davis SD (1994) Conduit diameter and drought-induced embolism in *Salvia mellifera* Greene (Labiatae). New Phytol 126:695–705.

Hacke UG, Sperry JS (2003) Limits to xylem refilling under negative pressure in *Laurus nobilis* and *Acer negundo*. Plant Cell Environ 26: 303–311.

Holbrook NM, Ahrens ET, Burns MJ, Zwieniecki MA (2001) In vivo observation of cavitation and embolism repair using magnetic resonance imaging. Plant Physiol 126:27–31.

Jansen S, Choat B, Pletsers A (2009) Morphological variation of intervessel pit membranes and implications to xylem function in angiosperms. Am J Bot 96:409–419.

Kluepfel DA, Aradhya MK, Browne GT, McKenry MV, Leslie CA, McClean AE, Moersfelder J, Velasco D, Baumgartner K (2012) The quest to identify disease resistance in the USDA-ARS *Juglans* germplasm collection. Acta Hortic 948:105–111.

Knipfer T, Fricke W (2010) Root pressure and a solute reflections coefficient close to unity exclude a purely apoplastic pathway of radial water transport in barley (*Hordeum vulgare* L.). New Phytol 187: 159–170.

Knipfer T, Eustis A, Brodersen C, Walker AM, McElrone AJ (2015*a*) Grapevine species from varied native habitats exhibit differences in embolism formation/repair associated with leaf gas exchange and root pressure. Plant Cell Environ 38:1503–1513.

Knipfer T, Brodersen CR, Amr Z, Kuepfel DA, McElrone AJ (2015*b*) Patterns of drought-induced embolism formation and spread in living walnut saplings visualized using x-ray microtomography. Tree Physiol 35:744–755.

Knipfer T, Cuneo IF, Brodersen CR, McElrone AJ (2016) In situ visualization of the dynamics in xylem embolism formation and removal in the absence of root pressure: a study on excised grapevine stems. Plant Physiol 171:1024–1036.

Knipfer T, Cuneo IF, Earles JM, Reyes C, Brodersen CR, McElrone AJ (2017) Storage compartments for capillary water rarely refill in an intact woody plant. Plant Physiol 175:1649–1160.

Lens F, Sperry JS, Christman MA, Choat B, Rabaey D, Jansen S (2011) Testing hypotheses that link wood anatomy to cavitation resistance and hydraulic conductivity in the genus *Acer*. New Phytol 190: 709–723.

Martorell S, Diaz-Espejo A, Medrano H, Ball MC, Chaot B (2013) Rapid hydraulic recovery in *Eucalyptus pauciflora* after drought: linkages between stem hydraulics and leaf gas exchange. Plant Cell Environ 37: 617–626.

McCulloh K, Johnson DM, Meinzer FC, Voelker SL, Lachenbruch B, Domec JC (2012) Hydraulic architecture of two species differing in wood density: opposing strategies in co-occurring tropical pioneer species. Plant Cell Environ 35:116–125.

McElrone AJ, Choat B, Parkinson DY, MacDowell AA, Brodersen CR (2013) Using high resolution computed tomography to visualize the three dimensional structure and function of plant vasculature. J Vis Exp. doi:10.3791/50162.

Sakr S, Alvers G, Morillon R, Maurel K, Decourteix M, Guilliot A, Fleurat-Lessard P, Julien JL, Chrispeels MJ (2003) Plasma membrane aquaporins are involved in winter embolism recovery in walnut tree. Plant Physiol 133:630–641.

Salleo S, Trifilo P, Lo Gullo MA (2008) Vessel wall vibrations: trigger for embolism repair. Funct Plant Biol 35:289–297.

Scholz A, Klepsch M, Karimi Z, Jansen S (2013) How to quantify conduits in wood? Front Plant Sci 4:1–11.

Secchi F, Zwieniecki MA (2013) Sensing embolism in xylem vessels: the role of sucrose as a trigger for refilling. Plant Cell Environ 34: 514–524.

Sparks JP, Black RA (1999) Regulation of water loss in populations of *Populus trichocarpa*: the role of stomatal control in preventing xylem cavitation. Tree Physiol 19:453–459.

Torres-Ruiz JM, Jansen S, Choat B et al. (2015) Direct x-ray microtomography observation confirms the induction of embolism upon xylem cutting under tension. Plant Physiol 167:40–43.

Tyree MT, Sperry JS (1989) Vulnerability of xylem to cavitation and embolism. Annu Rev Plant Physiol Plant Mol Biol 40:19–38.

Tyree MT, Cochard H, Cruiziat P, Sinclair B, Ameglio T (1993) Drought-induced leaf shedding in walnut: evidence for vulnerability segmentation. Plant Cell Environ 16:879–882.

Wegner LH (2013) Root pressure and beyond: energetically uphill water transport into xylem vessels? J Exp Bot 65:381–393.

Wheeler JK, Sperry JS, Hacke UG, Hoang N (2005) Inter-vessel pitting and cavitation in woody rosaceae and other vesselled plants: a basis for a saftey vs. efficiency trade-off in xylem transport. Plant Cell Environ 28:800–812.

Wheeler JK, Huggett BA, Tofte AN, Rockwell FE, Holbrook NM (2013) Cutting xylem under tension or supersaturated with gas can generate PLC and the appearance of rapid recovery from embolism. Plant Cell Environ 36:1938–1949.